

ANL-76-43

DL-273

ANL-76-43

167/18.76  
9-18-76

USE OF KRYPTON-85 FOR  
THE DETECTION OF PINHOLE FAILURES  
IN GCFR CLADDING

by

F. L. Yaggee, A. Purohit,  
and R. B. Poeppel



U of C AIA-USERDA

---

ARGONNE NATIONAL LABORATORY, ARGONNE, ILLINOIS

Operated for the U. S. ENERGY RESEARCH  
AND DEVELOPMENT ADMINISTRATION  
under Contract W-31-109-Eng-38

MASTER

## **DISCLAIMER**

**This report was prepared as an account of work sponsored by an agency of the United States Government. Neither the United States Government nor any agency Thereof, nor any of their employees, makes any warranty, express or implied, or assumes any legal liability or responsibility for the accuracy, completeness, or usefulness of any information, apparatus, product, or process disclosed, or represents that its use would not infringe privately owned rights. Reference herein to any specific commercial product, process, or service by trade name, trademark, manufacturer, or otherwise does not necessarily constitute or imply its endorsement, recommendation, or favoring by the United States Government or any agency thereof. The views and opinions of authors expressed herein do not necessarily state or reflect those of the United States Government or any agency thereof.**

## **DISCLAIMER**

**Portions of this document may be illegible in electronic image products. Images are produced from the best available original document.**

The facilities of Argonne National Laboratory are owned by the United States Government. Under the terms of a contract (W-31-109-Eng-38) between the U. S. Energy Research and Development Administration, Argonne Universities Association and The University of Chicago, the University employs the staff and operates the Laboratory in accordance with policies and programs formulated, approved and reviewed by the Association.

#### MEMBERS OF ARGONNE UNIVERSITIES ASSOCIATION

The University of Arizona  
Carnegie-Mellon University  
Case Western Reserve University  
The University of Chicago  
University of Cincinnati  
Illinois Institute of Technology  
University of Illinois  
Indiana University  
Iowa State University  
The University of Iowa

Kansas State University  
The University of Kansas  
Loyola University  
Marquette University  
Michigan State University  
The University of Michigan  
University of Minnesota  
University of Missouri  
Northwestern University  
University of Notre Dame

The Ohio State University  
Ohio University  
The Pennsylvania State University  
Purdue University  
Saint Louis University  
Southern Illinois University  
The University of Texas at Austin  
Washington University  
Wayne State University  
The University of Wisconsin

#### NOTICE

This report was prepared as an account of work sponsored by the United States Government. Neither the United States nor the United States Energy Research and Development Administration, nor any of their employees, nor any of their contractors, subcontractors, or their employees, makes any warranty, express or implied, or assumes any legal liability or responsibility for the accuracy, completeness or usefulness of any information, apparatus, product or process disclosed, or represents that its use would not infringe privately-owned rights. Mention of commercial products, their manufacturers, or their suppliers in this publication does not imply or connote approval or disapproval of the product by Argonne National Laboratory or the U. S. Energy Research and Development Administration.

Printed in the United States of America  
Available from  
National Technical Information Service  
U. S. Department of Commerce  
5285 Port Royal Road  
Springfield, Virginia 22161  
Price: Printed Copy \$3.50; Microfiche \$2.25

Distribution Category:  
Gas Cooled Reactor Technology  
(UC-77)

ANL-76-43

ARGONNE NATIONAL LABORATORY  
9700 South Cass Avenue  
Argonne, Illinois 60439

NOTICE  
This report was prepared as an account of work sponsored by the United States Government. Neither the United States nor the United States Energy Research and Development Administration, nor any of their employees, nor any of their contractors, subcontractors, or their employees, makes any warranty, express or implied, or assumes any legal liability or responsibility for the accuracy, completeness or usefulness of any information, apparatus, product or process disclosed, or represents that its use would not infringe privately owned rights.

USE OF KRYPTON-85 FOR  
THE DETECTION OF PINHOLE FAILURES  
IN GCFR CLADDING

by

F. L. Yaggee, A. Purohit,  
and R. B. Poeppel

Materials Science Division

May 1976

MASTER

EX  
DISTRIBUTION OF THIS DOCUMENT IS UNLIMITED

THIS PAGE  
WAS INTENTIONALLY  
LEFT BLANK

## TABLE OF CONTENTS

	<u>Page</u>
ABSTRACT . . . . .	5
I. INTRODUCTION . . . . .	5
II. USE OF KRYPTON-85 IN GCFR CLADDING STUDIES . . . . .	5
III. KRYPTON-85 CONCENTRATIONS . . . . .	7
IV. EFFLUENT GAS ACTIVITY . . . . .	9
APPENDIXES	
A. Gas Flow through an Orifice . . . . .	12
B. Krypton-85 Decay Constant . . . . .	13
C. System-volume Relations . . . . .	14
ACKNOWLEDGMENTS . . . . .	18
REFERENCES . . . . .	19

MASTER

## LIST OF FIGURES

<u>No.</u>	<u>Title</u>	<u>Page</u>
1.	Schematic of Gas Flow through GCFR Cladding Test Equipment . . . . .	6
2.	Volume Relations in GCFR Cladding Test Equipment. . . . .	15
3.	Viscosities of Noble Gases . . . . .	15
4.	Maximum $^{85}\text{Kr}$ Flow Rate as a Function of Total Pressure for a Mixture of Helium and 0.3 ppm $^{85}\text{Kr}$ . . . . .	16
5.	Flow Rates of Helium and $^{85}\text{Kr}$ for a Gas Mixture Discharging through an Orifice with a Diameter of $2.54 \times 10^{-3}$ cm . . . . .	16
6.	Volumes of Helium and $^{85}\text{Kr}$ Released by a Gas Mixture Discharging through an Orifice with a Diameter of $2.54 \times 10^{-3}$ cm . . . . .	17
7.	Flow Rates of Helium and $^{85}\text{Kr}$ for a Gas Mixture Discharging through an Orifice with a Diameter of $7.87 \times 10^{-2}$ cm . . . . .	17
8.	Volumes of Helium and $^{85}\text{Kr}$ Released by a Gas Mixture Discharging through an Orifice with a Diameter of $7.87 \times 10^{-2}$ cm . . . . .	17

USE OF KRYPTON-85 FOR  
THE DETECTION OF PINHOLE FAILURES  
IN GCFR CLADDING

by

F. L. Yaggee, A. Purohit,  
and R. B. Poeppel

ABSTRACT

Radioactive  $^{85}\text{Kr}$  is used as a tracer to detect pinhole failures in GCFR cladding. High-purity helium (99.99% pure) that contains 0.3 ppm  $^{85}\text{Kr}$  is used to pressurize the tubular test specimens, and a Geiger-Mueller counter is used to detect  $^{85}\text{Kr}$  in the helium environmental gas as it leaves the test chamber. Under the least favorable conditions of temperature and specimen pressure ( $760^\circ\text{C}$  and 35.6 atm), it is estimated that the smallest pinhole failure that could be detected within 60 s would have an orifice diameter of 0.0102 cm ( $\sim 102 \mu\text{m}$ ). Using lead shielding around the Geiger-Mueller counter to reduce background radiation, the electronics associated with the  $^{85}\text{Kr}$  detector will terminate a biaxial creep test at  $^{85}\text{Kr}$  activity levels above 20 counts/min.

I. INTRODUCTION

The purpose of the present report is fivefold: (a) to describe the use of radioactive krypton ( $^{85}\text{Kr}$ ) for the detection of pinhole failures in GCFR cladding, (b) to inform interested and affected parties of plans to use  $^{85}\text{Kr}$  in Room CL-103 of Building 212 at Argonne National Laboratory, (c) to acquaint all parties of the manner in which the  $^{85}\text{Kr}$  will be used and exhausted to the building stack, (d) to define the minimum  $^{85}\text{Kr}$  concentration required for the intended application, and (e) to present data in support of the view that the quantities involved and the method of discharge will not exceed ERDA standards for the maximum permissible concentration (mpc) of  $^{85}\text{Kr}$  in air. On the basis of the information presented, it is proposed that the quantities of  $^{85}\text{Kr}$  to be used will not adversely affect ANL personnel working in the immediate vicinity of Room CL-103 nor be detrimental to the general public.

II. USE OF KRYPTON-85 IN GCFR CLADDING STUDIES

High-purity helium tagged with parts-per-million quantities of  $^{85}\text{Kr}$  will be used to internally pressurize tube specimens during the mechanical-property

studies of Gas-Cooled Fast Reactor (GCFR) cladding. Short-term burst and long-term biaxial creep tests will be conducted in a helium environment flowing at a volume rate of 400 cc/min. These tests will encompass a temperature range between 538 and 760°C, and the specimens will be subjected to internal pressures between 526 and 7853 psig. The test apparatus was used in similar studies on Liquid Metal Fast Breeder Reactor (LMFBR) cladding and has been described in detail elsewhere.<sup>1</sup> A simplified representation of the overall test system is shown in Fig. 1.

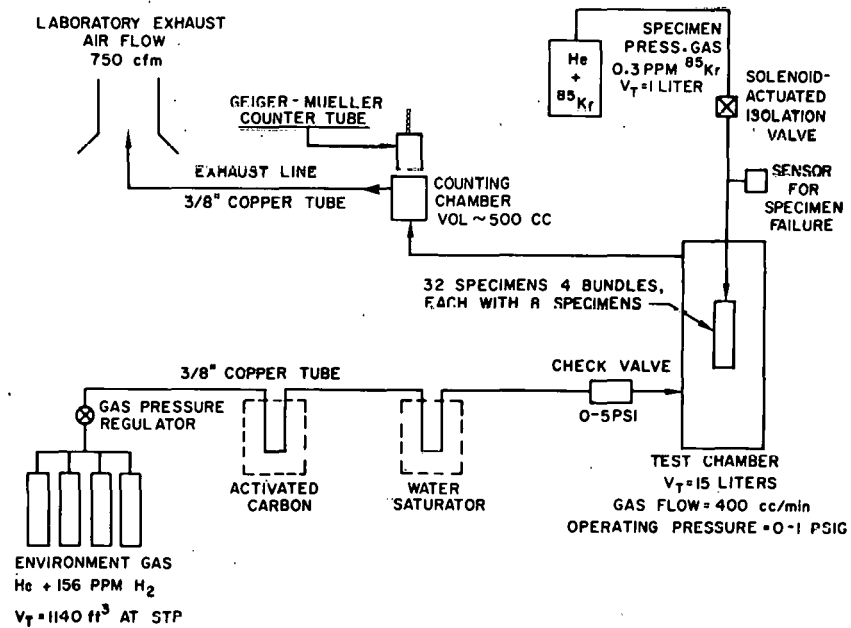


Fig. 1. Schematic of Gas Flow through GCFR Cladding Test Equipment. Neg. No. MSD-62620.

The test apparatus accommodates 32 specimens arranged in four bundles or clusters, each containing eight specimens. The eight specimens of one bundle are attached to a common manifold and are pressurized simultaneously from a 1-liter, high-pressure gas-storage vessel. Each specimen bundle is pressurized from a different gas-storage vessel, and each pressurizing system contains a pressure gauge with electrical contacts. When specimen failure results in a drop in pressure, the closing of the electrical contacts actuates the solenoid valve in the pressurizing line, which automatically isolates the specimen bundle from its high-pressure gas source. When specimen failure by wall perforation is so small that  $^{85}\text{Kr}$  can leak out without a drop in specimen pressure, the Geiger-Mueller (G-M) counter in the effluent gas stream will detect the  $^{85}\text{Kr}$  activity and also initiate the closing of the solenoid isolation valve. Therefore, the  $^{85}\text{Kr}$  tracer released to the test chamber will be exhausted to the building stack through a 3/8-in.-outside-diameter (OD) copper exhaust line.

The environmental gas is commercial high-purity helium that contains a maximum of 156 ppm H<sub>2</sub>. It is supplied by four gas bottles, each at 2640 psig

pressure, and each contains  $\sim 285 \text{ ft}^3$  (8067 liters) of gas at standard temperature and pressure (STP) conditions. The environmental gas contains a maximum of 38 ppm  $\text{H}_2\text{O}$  before it enters the test chamber through a 3/8-in.-OD copper line. A regulated supply-line pressure of 5-20 psig is expected to produce the 400-cc/min gas flow rate through the test chamber, which will operate at or near atmospheric pressure (0-10 in. of  $\text{H}_2\text{O}$ ). The check valve in the supply line will prevent back-pressure surges and possible  $^{85}\text{Kr}$  flow toward the environmental gas supply.

The 156 ppm of  $\text{H}_2$  in the environmental helium gas is well below the 8%  $\text{H}_2$  concentration that has been found inherently safe with respect to explosion hazard when mixed with air in all proportions.<sup>2,3</sup> The subsequent addition of 38 ppm  $\text{H}_2\text{O}$  is not expected to adversely affect the inherently safe character of the environmental gas mixture. Argon- $\text{H}_2$  mixtures will be avoided because of the potential explosion hazard identified with certain  $\text{H}_2$  concentrations.<sup>4</sup>

The bottles of helium gas that supply the gas environment will be replenished in pairs to avoid unscheduled test interruptions. The depletion rate of gas-bottle pairs at a gas flow rate of 400 cc/min will be

$$(2 \times 8067 \times 2525/2600) \div (0.4 \times 60 \times 24) = 27 \text{ days.}$$

Therefore, the environmental gas bottles will be replaced in pairs at 27-day intervals.

### III. KRYPTON-85 CONCENTRATIONS

Test specimens will be pressurized with a helium- $^{85}\text{Kr}$  gas mixture that contains 0.3 ppm  $^{85}\text{Kr}$  supplied by a standard gas cylinder at 2200 psig pressure. The total gas volume at STP is  $213 \text{ ft}^3$  (6029 liters). The 2.7-Ci activity level of the cylinder will be below the 3-Ci/cylinder activity limit imposed by transportation regulations. All quantities of  $^{85}\text{Kr}$  released to the test chamber will be exhausted, with the environmental gas, to the atmosphere through the building stack. The rationale and the calculation methods used in this assessment are given in Appendixes A-C and Figs. 2-8 (in Appendix C).

Figure 4 shows the initial or maximum  $^{85}\text{Kr}$  flow rates as a function of total pressure for two orifice sizes. These data assume a 0.3-ppm  $^{85}\text{Kr}$  concentration in helium and encompass the temperature and pressure ranges of interest, namely, 538-760°C and 523-7853 psig. Pinhole-type cladding failures are simulated by orifice diameters of  $2.54 \times 10^{-4}$  and  $2.54 \times 10^{-3}$  cm. (Hereafter, to facilitate calculations, specimen pressures will be given in atmospheres or dynes/cm<sup>2</sup>.\* Data in Fig. 4 indicate that, for a given orifice size ( $2.54 \times 10^{-3}$  cm), the greatest difficulty encountered in the detection of pinhole-type specimen failures will be at the lowest specimen pressure and the highest

\*1 atm = 14.696 psi =  $1.0132 \times 10^6$  dynes/cm<sup>2</sup>.

specimen temperature. Since cladding failure by violent rupture is often preceded by a pinhole leak, rapid detection of the smallest pinhole leak is important to the study of failure mechanisms.<sup>5</sup> In all the following calculations, rapid and complete mixing is assumed between the <sup>85</sup>Kr released from the specimen and the environmental gas in the test chamber.

Figure 5 shows that, at 760°C and a specimen pressure of 35.6 atm, the <sup>85</sup>Kr flow rate through an orifice with a diameter of  $2.54 \times 10^{-3}$  cm remains essentially constant for the first 1000 s and then begins to decrease appreciably. Figure 6 indicates that the volume release of helium and <sup>85</sup>Kr to the test chamber through a cladding pinhole failure of the same orifice size is also constant during the first 1000 s. Since the flow rate of the environmental gas past the G-M counter located in the effluent gas stream is 400 cc/min, the <sup>85</sup>Kr released to the test chamber will be swept past the detector at the same rate.

The capability of the G-M counter to detect a specimen failure of this size depends upon the concentration of <sup>85</sup>Kr passing the counter per minute and the counter efficiency. The latter is affected by the estimated 50% areal transparency of the stainless steel window in the counting chamber ( $5.08 \times 10^{-3}$  cm in diameter by  $7.62 \times 10^{-3}$  cm thick) and the efficiency with which the counter is shielded against normal background radiation. For a totally unshielded counter, the normal background radiation produces ~200-400 counts/min. The gas-exhaust system is constructed so that 100% of the effluent gas stream passes the G-M counter.

Figure 6 shows that  $3.1 \times 10^{-8}$  liter of <sup>85</sup>Kr and  $6.5 \times 10^{-2}$  liter of helium will be released to the test chamber during the first 60 s through a pinhole failure with an orifice diameter of  $2.54 \times 10^{-3}$  cm when a specimen is pressurized to 35.6 atm. Since both these volumes are small compared with the 15-liter test-chamber volume, <sup>85</sup>Kr dilution will be determined solely by the volume of the test chamber. The activity of the <sup>85</sup>Kr released to the test chamber and the capability of the G-M counter to detect the activity can be determined by using the decay constant for <sup>85</sup>Kr from Appendix B [ $\lambda = 1.22791 \times 10^{-7}$  disintegration per minute (dpm)/atom <sup>85</sup>Kr].

(a) Activity of <sup>85</sup>Kr released to the test chamber in 60 s

$$[{}^{85}\text{Kr} (\text{liters}) \times \lambda \times 6.03 \times 10^{23}] \div 22.4 = \text{dpm}$$

$$(3.1 \times 10^{-8} \times 1.22791 \times 10^{-7} \times 6.03 \times 10^{23}) \div 22.4 = 1.02 \times 10^8 \text{ dpm.}$$

(b) Concentration of <sup>85</sup>Kr in the test chamber in 60 s

$${}^{85}\text{Kr activity} \times \text{dilution factor} = \text{dpm/liter}$$

$$(1.02 \times 10^8) \times (3.1 \times 10^{-8} \div 15) = 2.11 \times 10^{-1} \text{ dpm/liter.}$$

(c) Activity  $^{85}\text{Kr}$  passing G-M counter in 60 s

$$^{85}\text{Kr} \text{ concentration} \times \text{flow rate} = \text{dpm}$$

$$2.11 \times 10^{-1} \times 0.4 = 8.44 \times 10^{-2} \text{ dpm.}$$

Considering a 50% areal transparency of the window in the counting chamber, the  $^{85}\text{Kr}$  activity detected by the G-M counter will be  $0.5 \times 8.44 \times 10^{-2} = 4.22 \times 10^{-2}$  dpm. This level of activity would not be detected by the G-M counter, even when the counter is heavily shielded. (A 2-in.-thick lead shield around the G-M counter is expected to reduce background radiation to ~10 counts/min.) Since a factor-of-10 increase in orifice size produces a  $10^4$  increase in flow rate (Fig. 4), the diameter of the smallest pinhole failure detected within 60 s under least favorable conditions of temperature and specimen pressure (Figs. 5 and 6) is estimated to be  $\sim 1.02 \times 10^{-2}$  cm. The  $^{85}\text{Kr}$  activity released by an orifice of this size and detected by the G-M counter is given by  $(R_2^4 \div R_1^4) \times 4.22 \times 10^{-2}$  dpm, where  $R_1$  and  $R_2$  are the radii of the orifice. Thus, the  $^{85}\text{Kr}$  activity detected by the G-M counter during the first 60 s after the pinhole failure occurs is

$$\frac{1.06 \times 10^{-9}}{2.601 \times 10^{-12}} \times 4.22 \times 10^{-2} = 17.2 \text{ dpm.}$$

The mpc level for  $^{85}\text{Kr}$  discharged to the atmosphere is limited to  $6.66 \times 10^2$  dpm/liter by ERDA regulations.<sup>6</sup> Using a  $2.12 \times 10^4$  ventilator dilution factor<sup>7</sup> (750-cfm airflow) and a  $10^5$  stack dilution factor,<sup>8</sup> the  $^{85}\text{Kr}$  concentration exhausted to the stack, and subsequently to the atmosphere within the Laboratory perimeter, in the first 60 s will be:

(a) Stack

$$[17.2 \text{ (dpm)} \div (\text{flow rate})] \times \text{ventilator dilution}$$

$$(17.2 \div 0.4) \times 2.12 \times 10^{-4} = 9.11 \times 10^{-3} \text{ dpm/liter.}$$

(b) Atmosphere within Laboratory perimeter

$$9.11 \times 10^{-3} \times 1 \times 10^{-5} = 9.11 \times 10^{-8} \text{ dpm/liter.}$$

These quantities are  $1.37 \times 10^{-6}$  and  $1.37 \times 10^{-10}$  mpc, respectively, and remain essentially constant for 1000 s and then decrease (Figs. 5 and 6). Therefore, the release of these concentrations of  $^{85}\text{Kr}$  to the atmosphere are of no consequence to the environment.

## IV. EFFLUENT GAS ACTIVITY

The largest  $^{85}\text{Kr}$  concentrations exhausted to the atmosphere with the effluent gas stream will occur after simultaneous failure by violent rupture

of several specimens in each of the four specimen bundles and by malfunction of the isolation valve in each pressurizing system (Fig. 2). Should these unlikely events occur, the entire gas mixture of high-pressure helium and 0.3 ppm  $^{85}\text{Kr}$  in each of the four storage vessels will discharge into the test chamber. The depressurization of a single gas-storage vessel at an initial pressure of 534.36 atm is characterized by the curves in Figs. 7 and 8. The chronology of events during such rapid depressurization is expected to be as follows.

The high flow rate that results from the sudden release of the helium- $^{85}\text{Kr}$  gas mixture will cause the check valve in the environmental gas supply line to close and prevent back-streaming of  $^{85}\text{Kr}$  to the environmental gas source. Since the test chamber operates essentially at atmospheric pressure, the discharging gas will exhaust continuously to the stack. Assuming each of the four storage vessels are at the maximum pressure of 534.36 atm when the event occurs, the discharges of helium and  $^{85}\text{Kr}$  to the stack can be determined by means of Figs. 7 and 8. Figure 7 shows that flow rates for helium and  $^{85}\text{Kr}$  will be  $5.2 \times 10^3$  and  $3.2 \times 10^{-3}$  cc/s, respectively, and will remain relatively constant for the first 60 s of the depressurization. Depressurization is complete in  $\sim 420$  s ( $\sim 7$  min). Furthermore, the volume of helium discharged from each storage vessel is larger by a factor of 345 than the test chamber volume; therefore, the  $^{85}\text{Kr}$  dilution factor is essentially that represented by the gas mixture of helium and 0.3 ppm  $^{85}\text{Kr}$ .

The volumes of helium and  $^{85}\text{Kr}$  released to the room ventilator duct will be a maximum during the first 60 s of depressurization and then will decrease significantly over the succeeding 3600 s (60 min), as indicated in Fig. 7. Figure 8 shows that the volumes of helium and  $^{85}\text{Kr}$  released from each storage vessel to the room-ventilator duct during the first 60 s will be  $2.5 \times 10^2$  and  $5.6 \times 10^{-5}$  liters, respectively, and the helium dilution factor will be the ratio of these volumes ( $2.24 \times 10^{-7}$ ).

(a)  $^{85}\text{Kr}$  activity at the ventilator duct in 60 s

$$(4 \times 5.6 \times 10^{-5} \times 6.03 \times 10^{23} \times 1.22791 \times 10^{-7}) \div 22.4 = \\ 7.40 \times 10^{11} \text{ dpm.}$$

(b)  $^{85}\text{Kr}$  concentration at the ventilator duct in 60 s

$$(7.40 \times 10^{11} \div 0.4) \times 2.24 \times 10^{-7} \times 2.12 \times 10^{-4} = \\ 8.78 \times 10^1 \text{ dpm/liter} \approx 1.3 \times 10^{-1} \text{ mpc.}$$

(c)  $^{85}\text{Kr}$  concentration released to the atmosphere in 60 s

$$8.78 \times 10^1 \times 1 \times 10^{-5} = 8.78 \times 10^{-4} \text{ dpm/liter} \approx 1.3 \times 10^{-6} \text{ mpc.}$$

During the second 60 s of storage-vessel depressurization,  $\sim 6 \times 10^2$  liters of helium and  $1.68 \times 10^{-4}$  liter of  $^{85}\text{Kr}$  will be exhausted to the stack, and the helium dilution factor will be  $\sim 2.8 \times 10^{-7}$ . The  $^{85}\text{Kr}$  concentration released to the atmosphere will be  $8.06 \times 10^{-4}$  dpm/liter or  $1.21 \times 10^{-6}$  mpc. For all subsequent 1-min intervals to complete depressurization of all storage vessels, the amount of  $^{85}\text{Kr}$  released will diminish; therefore, the atmospheric concentration should never exceed or approach the  $6.66 \times 10^2$ -dpm/liter mpc set by ERDA regulations. Additional precautions will be taken to ensure safe utilization of the radioactive  $^{85}\text{Kr}$  gas species and will also include the following:

1. The entire system (Fig. 1) will be checked for helium tightness at pressures up to 15 psig. This will ensure complete containment of the  $^{85}\text{Kr}$  within the test apparatus before it is discharged to the stack.
2. No more than two storage vessels will be in operation at any one time at the maximum pressure of 534.36 atm.
3. Equipment operators and other personnel occupying Room CL-103 will be required to carry radiation monitors.
4. Air monitors will be used in Room CL-103 as recommended by the Building 212 radiation-safety representative.
5. All lines will be purged with 100% helium gas before the apparatus is opened at the conclusion of each test run or when a test run is interrupted.

## APPENDIX A

Gas Flow through an Orifice

It is assumed that helium and  $^{85}\text{Kr}$  flow rates through an orifice at elevated temperature are adequately represented by<sup>9</sup>

$$\text{Flow rate} = \frac{\pi P_d R^4}{8 \ell \eta} \text{ cc/s,} \quad (\text{A.1})$$

where

$P_d$  = pressure difference across orifice, in dynes/cm<sup>2</sup>;

$R$  = orifice radius, in centimeters;

$\ell$  = orifice length, in centimeters;

and

$\eta$  = gas viscosity, in poises.

Flow-rate calculations derived from Eq. A.1 assume that a circular orifice is an adequate simulation of a pinhole-type specimen failure. Since pinhole failures in LMFBR cladding occur at low diametral strains (~4%),<sup>5</sup> the orifice length ( $\ell$ ) is taken as  $4.389 \times 10^{-2}$  cm (~0.96 x specimen wall).

APPENDIX B  
Krypton-85 Decay Constant

Decay of any radioactive atom species is given by

$$N = N_0 \exp(-\lambda t), \quad (B.1)$$

where

$N_0$  = number of radioactive atoms at reference time  $t$ ;

$N$  = radioactive atoms after time  $\Delta t$ ;

and

$\lambda$  = decay constant, in dpm/atom.

Rewriting Eq. B.1 and setting  $N_0/N = 2$  when  $t_{1/2} = 10.74$  yr,  $\lambda$  is calculated as

$$\lambda = (\ln 2) / (10.74 \times 365 \times 24 \times 60),$$

or

$$\lambda = 1.22791 \times 10^{-7} \text{ dpm/atom}.$$

APPENDIX C  
System-volume Relations

A simplified representation of one of four specimen-pressurizing systems in the Mark-II Biaxial Creep Tester is shown in Fig. 2. During long-term biaxial creep tests, each of the four gas-storage vessels ( $V_{GS}$ ) operates at a different pressure ( $P_1 > P_2 > P_3 > P_4$ ) and each pressurizes a separate bundle of eight specimens. Approximately 100 in. of high-pressure tubing connects each specimen bundle to its high-pressure gas source. A solenoid-actuated valve isolates each specimen bundle from its high-pressure gas source when specimen failure has occurred. About 80-85% of the volume of each specimen is displaced with a solid slug to reduce the volume of high-pressure gas within the specimen. This approach eliminates deformation after specimen failure has occurred while the high-pressure gas is being dissipated.

Storage-vessel volume ( $V_{sv}$ ) 1 liter

Specimen volume ( $V_s$ ) 3.50 cc

Pressure-line volume ( $V_{pl}$ ) 1.24 cc

Displacement-slug volume ( $V_{ds}$ ) 2.87 cc

$$V_{sys} = V_{sv} + V_{pl} + (V_s - V_{ds}),$$

and

$$V_{sv} \approx 0.99 V_{sys},$$

where  $V_{sys}$  is the system volume. Ideal gas behavior is assumed for the helium-<sup>85</sup>Kr gas mixture, because both gas species have relatively low critical pressures ( $P_c$ ) and temperatures ( $T_c$ ).<sup>8</sup> (For helium,  $P_c = 2.26$  atm and  $T_c = -269.9^\circ\text{C}$ ; for <sup>85</sup>Kr,  $P_c = 54.3$  atm and  $T_c = -63.8^\circ\text{C}$ .)

The gas viscosity data in Fig. 3 (Ref. 9) and Eq. A.1 are used to calculate helium and <sup>85</sup>Kr flow rates (cc/s) and volumes (liters) released to the test chamber as a result of specimen failure or sudden depressurization following equipment malfunction. Maximum <sup>85</sup>Kr flow rates in a gas mixture that contains 0.3 ppm <sup>85</sup>Kr are plotted in Fig. 4 as a function of total system pressure. These data encompass the temperature range 538-760°C and the pressure range 35.6-534.36 atm for flow rates through orifices with diameters of  $2.54 \times 10^{-4}$  and  $2.54 \times 10^{-3}$  cm. Figure 4 shows that the <sup>85</sup>Kr flow rate (a) increases by a factor of 15 as the system pressure increases from 35.6 to 534.36 atm at constant temperature and orifice size, (b) decreases by a factor of 1.17 as the gas temperature increases from 538 to 760°C at constant system pressure and orifice size, and (c) increases by a factor of  $10^4$  for a factor-of-10 increase in orifice size, at constant gas temperature and pressure.

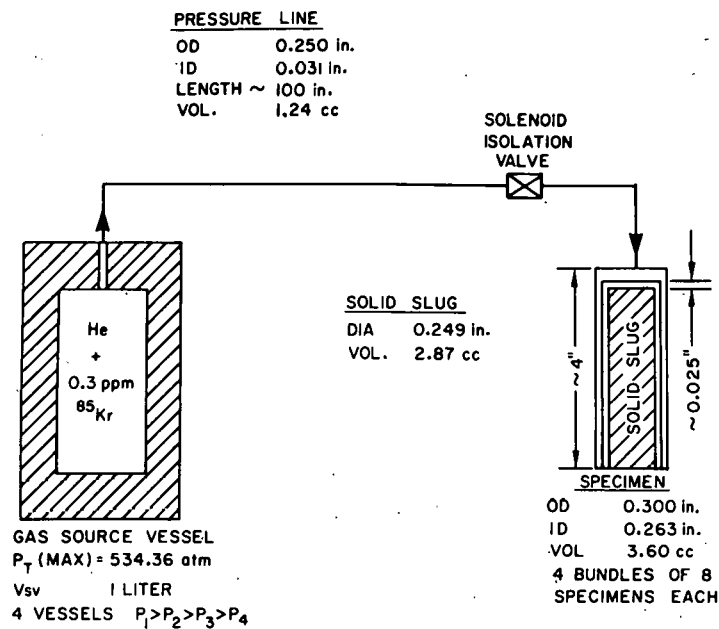


Fig. 2. Volume Relations in GCFR Cladding Test Equipment. Neg. No. MSD-62619.

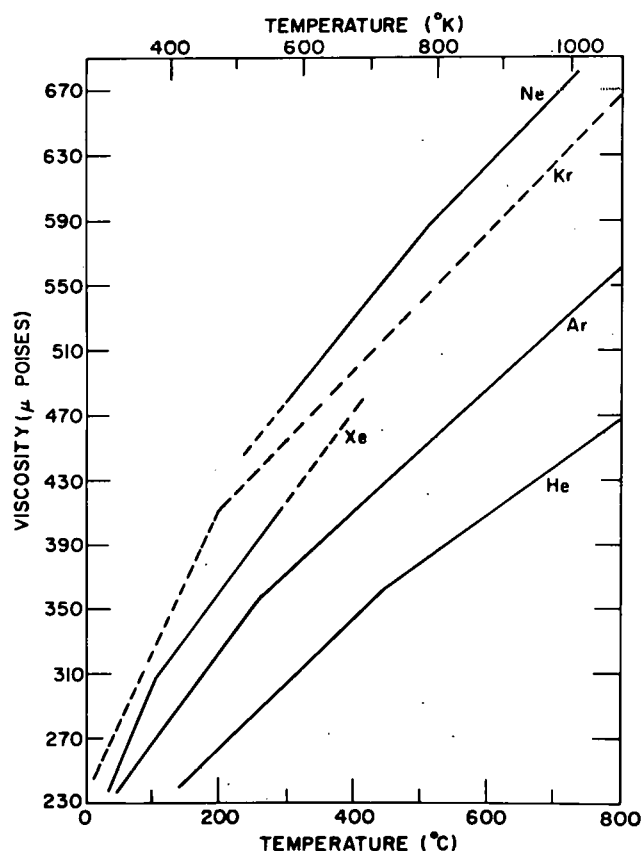


Fig. 3. Viscosities of Noble Gases.  
 Neg. No. MSD-62621.

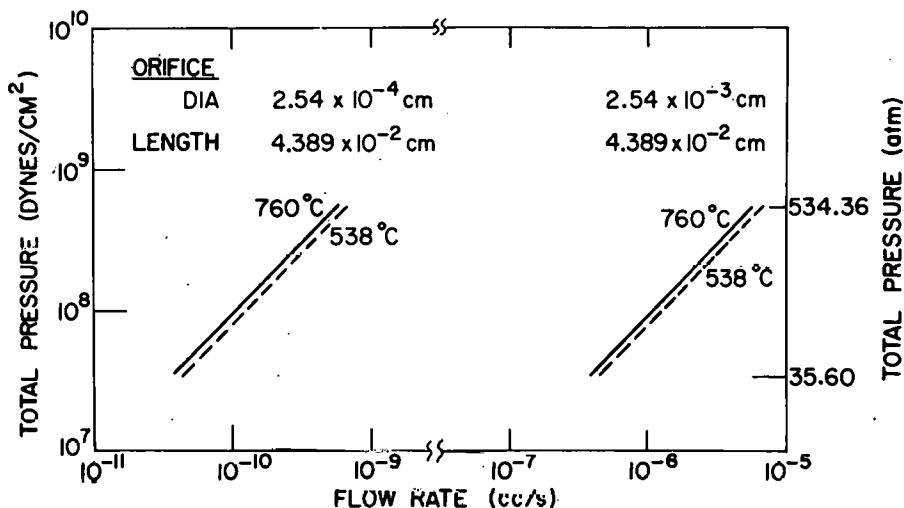


Fig. 4. Maximum  $^{85}\text{Kr}$  Flow Rate as a Function of Total Pressure for a Mixture of Helium and 0.3 ppm  $^{85}\text{Kr}$ . Neg. No. MSD-62622.

Figures 5 and 6 show the flow rates of helium and  $^{85}\text{Kr}$  and the volumes of both gases released as a function of time through a pinhole-type specimen failure simulated by an orifice with a diameter of  $2.54 \times 10^{-3}$  cm. These data are used to assess the capability of the G-M counter to detect pinhole-type specimen failures.

Figures 7 and 8 show the flow rates of helium and  $^{85}\text{Kr}$  and the volumes of both gas species released as a function of time during sudden depressurization following equipment malfunction. These data are used to assess the maximum level of  $^{85}\text{Kr}$  activity released to the atmosphere through the Building 212 stack.

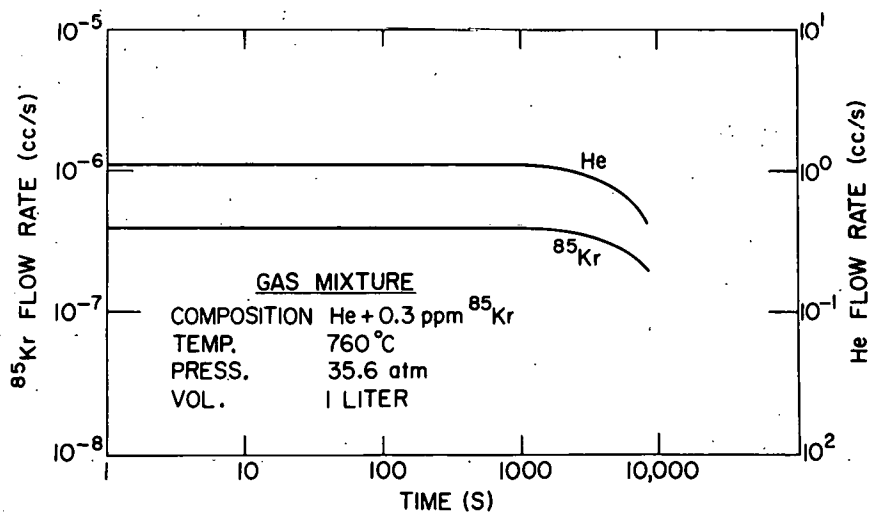


Fig. 5. Flow Rates of Helium and  $^{85}\text{Kr}$  for a Gas Mixture Discharging through an Orifice with a Diameter of  $2.54 \times 10^{-3}$  cm. Neg. No. MSD-62623.

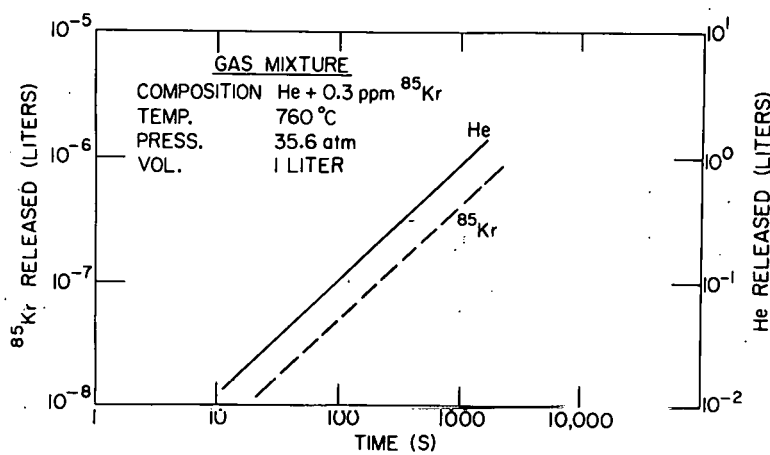


Fig. 6

Volumes of Helium and  $^{85}\text{Kr}$  Released by a Gas Mixture Discharging through an Orifice with a Diameter of  $2.54 \times 10^{-3}$  cm. Neg. No. MSD-62624.

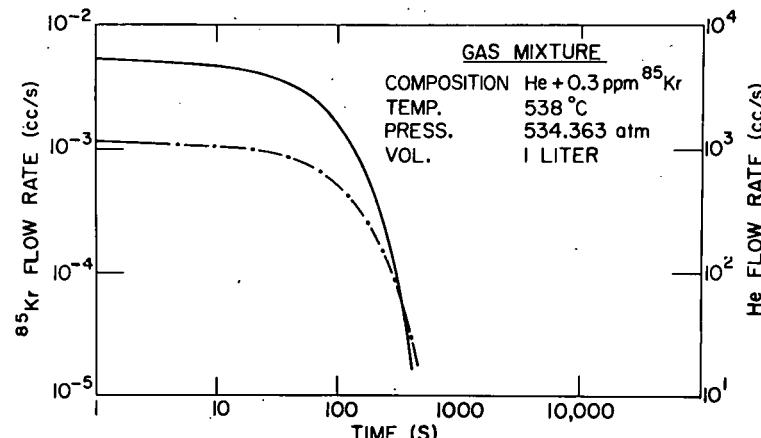


Fig. 7

Flow Rates of Helium and  $^{85}\text{Kr}$  for a Gas Mixture Discharging through an Orifice with a Diameter of  $7.87 \times 10^{-2}$  cm. Neg. No. MSD-62626.

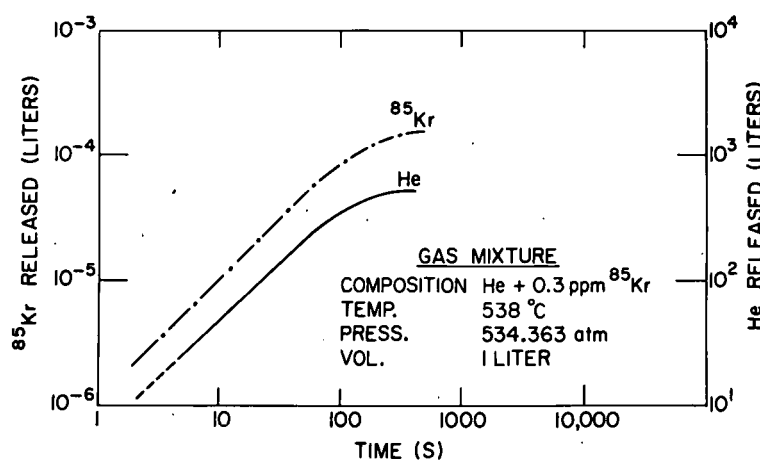


Fig. 8

Volumes of Helium and  $^{85}\text{Kr}$  Released by a Gas Mixture Discharging through an Orifice with a Diameter of  $7.87 \times 10^{-2}$  cm. Neg. No. MSD-62625.

### ACKNOWLEDGMENTS

We gratefully acknowledge the encouragement of R. W. Weeks and the help provided by the staff of the Materials Science Division in this work. A special expression of appreciation is due T. H. Braid of the Physics Division for the design and construction of the Geiger-Mueller counter tube and associated electronics and for his efforts toward the implementation of an electronic interface with the biaxial creep apparatus. Thanks are also due W. J. Grajek, who assembled the piping system that supplies the flowing-helium test environment, and to M. J. Robinet of the Occupational Health and Safety Division for his interest and help in the implementation of procedures for safe handling of radioactive gases.

## REFERENCES

1. F. L. Yaggee, J. W. Styles, and S. B. Brak, *Semiautomatic Apparatus for Creep and Stress-rupture Tests of Thin-wall Fuel-cladding Tubes under Internal Gas-pressure Loading*, ANL-7801 (Sept 1971).
2. C. L. Cheever, ANL, private communication (Feb 1975).
3. E. E. Voiland, Manager, Analytical Chemistry, ANL, memorandum to W. L. Delvin, Westinghouse Hanford Co., *Comments on RDT Standard F-11-1T* (Sept 28, 1973).
4. *Report of Incident at Gulf United Nuclear Plutonium Facility at Pawburg, New York*, Gulf United Nuclear Fuels Corp., Elmsford, N.Y. (Jan 28, 1972).
5. F. L. Yaggee and Che-Yu Li, *Failure Mechanisms for Internally Pressurized Thin-wall Tubes and Their Relationship to Fuel-element Failure Criteria*, ANL-7805 (Dec 1972).
6. AEC Manual, Chapter 0524, "Standards for Radiation Protection" (1973).
7. W. H. Livernash, ANL, private communication (1975).
8. M. J. Robinet, ANL, private communication (1975).
9. *CRC Handbook of Chemistry and Physics*, The Chemical Rubber Company, Cleveland, Ohio, 51st Edition (1970-1971).
10. J. H. Perry, *Chemical Engineer's Handbook*, 2nd Edition, McGraw-Hill, New York, pp. 474-477 (1941).